Supplemental material submitted for the paper:

**Evaluation of the carbon cycle components in the Norwegian Earth System Model (NorESM)**

J. F. Tjiputra, C. Roelandt, M. Bentsen, D. M. Lawrence, T. Lorentzen, J. Schwinger, Ø. Seland, and C. Heinze

In this supplemental document, we present some figures similar to those found in the main manuscript (Figs. 2, 3, 4, 6, 7, and 8), but representing data from the Bergen Earth System Model (BCM-C, Tjiputra et al., 2011). These figures mainly compare the BCM-C simulated ocean physical and biogeochemical tracers with those from observations. They are relevant to the manuscript because both the BCM-C and NorESM models adopt similar physical and biogeochemical ocean models (i.e., MICOM and HAMOCC5). It is important to note that there have been significant developments, particularly with respect the physical model, in the NorESM relative to the earlier BCM-C model. Nevertheless, these figures remain relevant and useful to reveal additional insight on the sensitivity of ocean biogeochemical tracers to the physical fields (e.g., circulation, temperature, etc.).

Supplemental figure s1 shows the statistical summary of BCM-C simulated ocean temperature, salinity, phosphate, dissolved oxygen, silicate, dissolved inorganic carbon, and alkalinity at different depths as compared to the observations. The model-data fit in temperature and salinity are generally reproduced in the NorESM model, though at 3000m depth, the model-data bias is higher in NorESM than in BCM-C. This bias is particularly pronounced in the North Atlantic deep water (see also Supplemental figure s2b and Fig. 3b in the manuscript), which is consistent with the strong AMOC simulated by NorESM. For the salinity field, the main difference between the two model is in the North Atlantic deep water, in which strong AMOC and large flux of saline water from the Mediterranean Sea in the NorESM model lead to salinity bias when compared to the observation.

With regards to nutrient concentration (e.g., phosphate), the NorESM simulates considerable improvement in the surface layer, predominantly in the Southern Ocean, North Pacific, North Atlantic, and equatorial Pacific. Figure s4 shows that the BCM-C uses up most of the available phosphate in these high productivity regions. We believe this is particularly as a result of improved mixing parameterization in the NorESM model. Consistently, the NorESM model also simulates higher annual mean primary production of $42.2\pm0.8$ Pg C yr$^{-1}$, as compared to $39.0\pm2.0$ Pg C yr$^{-1}$ simulated by the BCM-C model (Tjiputra et al, 2010). These differences is mostly associated with higher productivity in northern hemisphere high latitude.

The NorESM and BCM-C simulated surface dissolved oxygen are nearly identi-

cal as shown in Figs. 7a and s5a. However, considerable differences are simulated at deeper layer, predominantly within the Antarctic Bottom Water (AABW) in both the Atlantic and Pacific basins. The NorESM model tends to simulate more oxygen and less phosphate along these water masses relative to that in the BCM-C model. There are two factors which can explain this phenomena. First, the NorESM simulates stronger overturning circulation than the BCM-C. This leads to more surface oxygen exported into the deep bottom water (hence positive oxygen bias in NorESM). Secondly, the BCM-C model simulates larger net primary production (due to the bias in mixing, not shown here) than the NorESM, and therefore simulates more export production in this region. Analogously, larger Southern Ocean export production in BCM-C allows more organic carbon at depth available to be remineralized back to nutrient (i.e., larger phosphate concentration in BCM-C than in NorESM), which utilizes more oxygen, hence the lower oxygen in BCM-C.

Figure s6 shows the surface distribution of dissolved inorganic carbon (DIC) and alkalinity as simulated by the BCM-C model. Compared to the GLODAP datasets, the NorESM and BCM-C models tend to overestimate both the DIC and alkalinity. In the NorESM, the model-data bias is noticeably improved, especially for the surface alkalinity. This bias, as explains in the main manuscript, is not critical as approximately the difference between alkalinity and DIC determines the surface $pCO_2$, and hence the air-sea $CO_2$ flux. The models' alkalinity minus DIC fields are consistent with the observation.

Finally, figure s7 shows the evolution of several diagnostic parameters for the CTRL and HIST simulations from NorESM following a 900-years model spin up. Shown here are annual Atlantic meridional overturning circulation (AMOC) strength, annual net primary production, annual POC export, annual calcium carbonate export, annual opal export and dissolved oxygen inventory for the 1850–2005 period.

**References**

Antonov, J. I., Seidov, D., Boyer, T. P., Locarnini, R. A., Mishonov, A. V., Garcia, H. E., Baranova, O. K., Zweng, M. M., and Johnson, D. R.: World Ocean Atlas 2009, Volume 2: Salinity, edited by Levitus, S., NOAA Atlas NES-DIS 69, U.S. Government Printing Office, Washington, D.C., 184 pp., 2010.

Garcia, H. E., Locarnini, R. A., Boyer, T. P., Antonov, J. I., Baranova, O. K., Zweng, M. M., and Johnson, D. R.: World Ocean Atlas 2009, Volume 3: Dissolved Oxygen, Apparent Oxygen Utilization, and Oxygen Saturation, edited by Levitus, S., NOAA Atlas NESDIS 70, U.S. Government Printing Office, Washington, D.C., 344 pp., 2010a.

Garcia, H. E., Locarnini, R. A., Boyer, T. P., Antonov, J. I., Zweng, M. M., Baranova, O. K., and Johnson, D. R.: World Ocean Atlas 2009, Volume 4: Nutrients (phosphate, nitrate, silicate), edited by Levitus, S., NOAA Atlas NESDIS 71, U.S. Government Printing Office, Washington, D.C., 398 pp., 2010b.

Key, R. M., Kozyr, A., Sabine, C. L., Lee, K., Wanninkhof, R., Bullister, J. L., Feely, R. A., Millero, F. J., Mordy, C., and Peng, T.-H.: A global ocean carbon climatology: Results from Global Data Analysis Project (GLODAP), Global Biogeochem. Cy., 18, GB4031, doi:10.1029/2004GB002247, 2004.

Locarnini, R. A., Mishonov, A. V., Antonov, J. I., Boyer, T. P., Garcia, H. E., Baranova, O. K., Zweng, M. M., and Johnson D. R.: World Ocean Atlas 2009, Volume 1: Temperature, edited by Levitus, S., NOAA Atlas NESDIS 68, U.S. Government Printing Office, Washington, D.C., 184 pp, 2010.

Tjiputra, J. F., Assmann, K., Bentsen, M., Bethke, I., Otterå, O. H., Sturm, C., and Heinze, C.: Bergen Earth system model (BCM-C): model description and regional climate-carbon cycle feedbacks assessment, Geosci. Model Dev., 3, 123141, http://dx.doi.org/10.5194/gmd-3-123-2010doi:10.5194/gmd-3-123-2010, 2010.
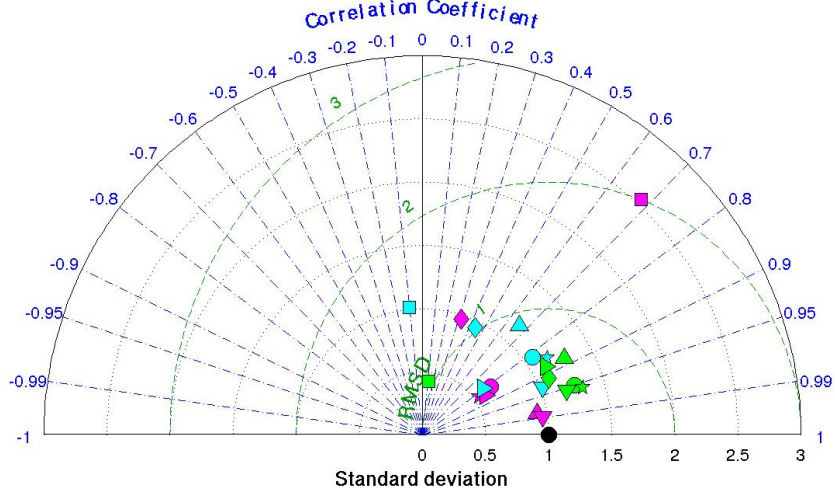
**Figure s1.** Taylor diagram of non-area weighted statistical summary between the BCM-C simulated and observed annually-averaged (climatology) of ($\bigtriangledown$) ocean temperature, ($\triangleright$) salinity, ($\star$) phosphate, ($\triangle$) dissolved oxygen, ($\bigcirc$) silicate, ($\diamond$) dissolved inorganic carbon, and ($\square$) alkalinity. Shown here are comparison at surface (magenta), 1000 meter (blue), and 3000 meter (green) depths. Observations are based on the World Ocean Atlas (WOA) and GLODAP (see also text). The black circle represents the observations. All standard deviations are normalized to the respected observed standard deviation. For temperature, salinity, phosphate, silicate and oxygen, we compare the HIST simulation from 1980–1999 period, whereas for DIC and ALK, we use the 1996–2005 simulation period.
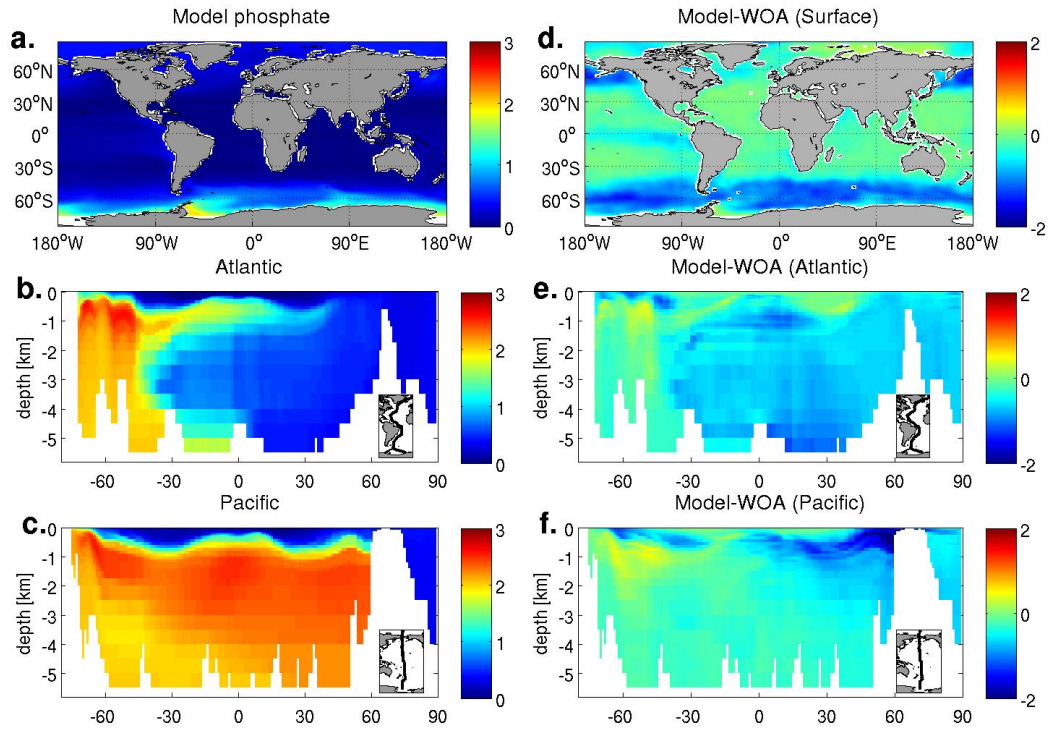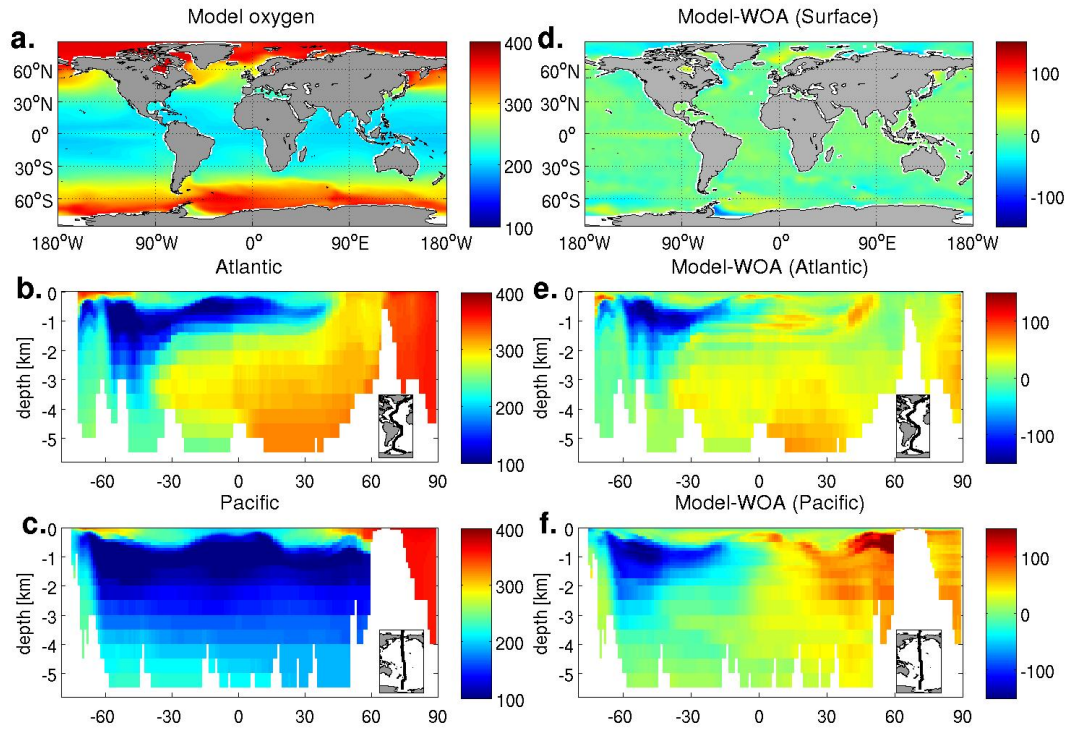
$\text{hist}_c trl_t s$
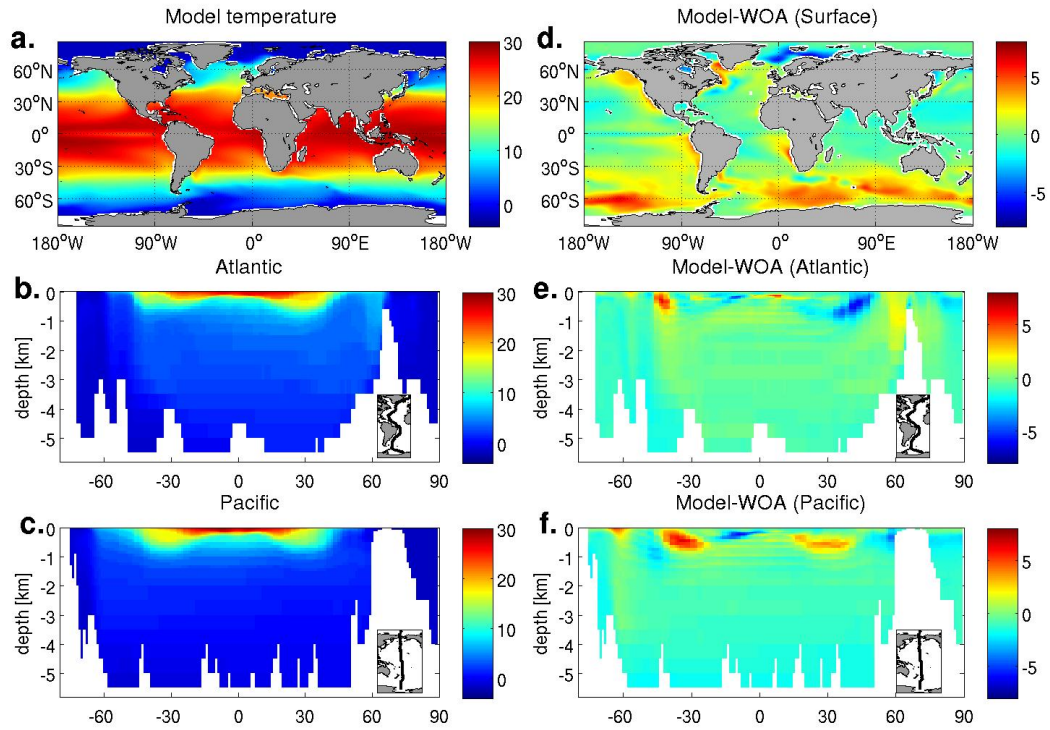
**Figure s2.** Distribution of ocean temperature from model simulation (left) and difference in temperature between the model and climatological estimates (right) (WOA, Locarnini et al., 2010) for the surface (a,d), Atlantic (b,e) and Pacific (c,f) vertical sections. Units are in [degree C].
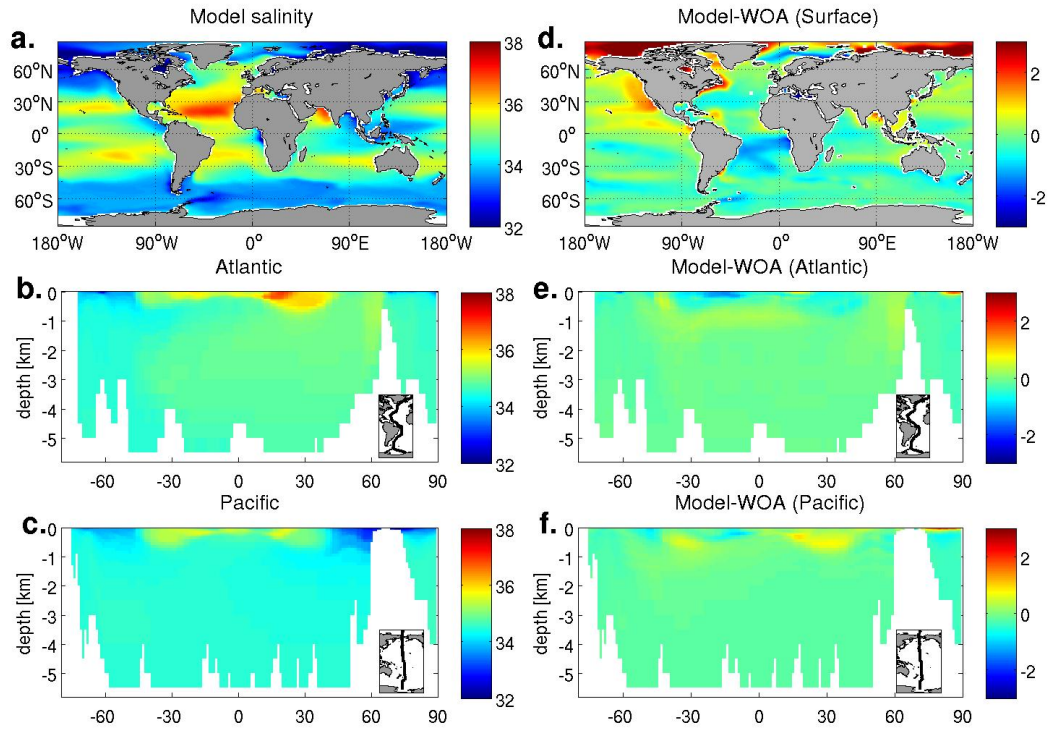
**Figure s3.** Distribution of ocean salinity from BCM-C model simulation (left) and difference in salinity between the model and climatological estimates (right) (WOA, Antonov et al., 2010) for the surface (a,d), Atlantic (b,e) and Pacific (c,f) vertical sections. Units are in [psu].

**Figure s4.** Distribution of dissolved phosphate concentration from BCM-C model simulation (left) and difference in phosphate between the model and climatological estimates (right) (WOA, Garcia et al., 2010b) for the surface (a,d), Atlantic (b,e) and Pacific (c,f) vertical sections. Units are in $[\mu\text{mol L}^{-1}]$.
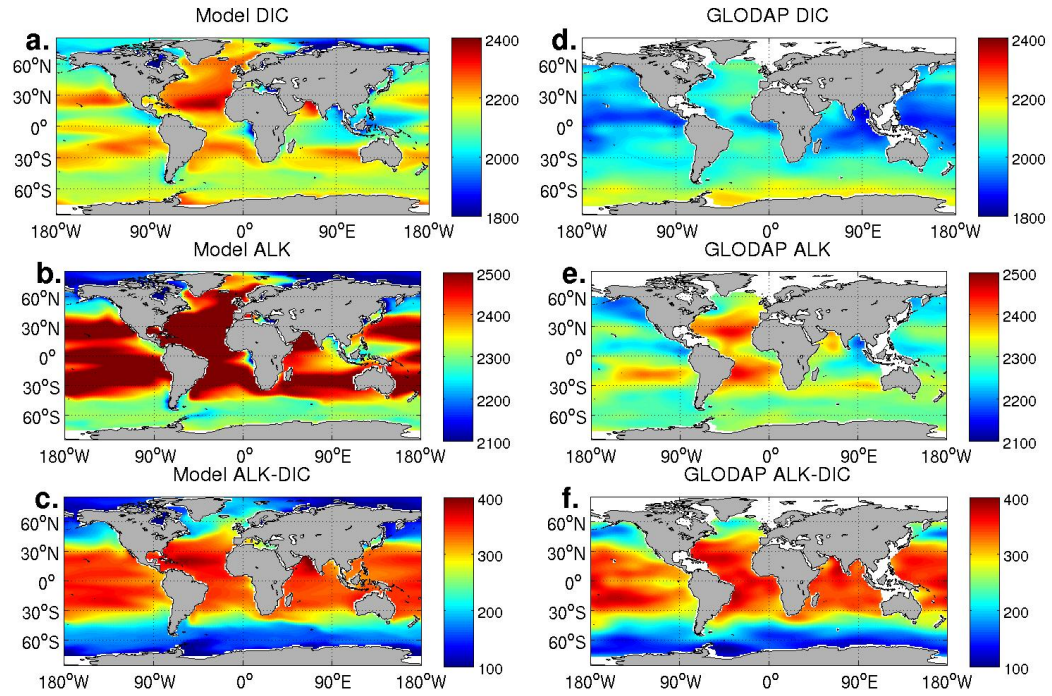
**Figure s5.** Distribution of dissolved oxygen concentration from BCM-C model simulation (left) and difference in oxygen between the model and climatological estimates (right) (WOA, Garcia et al., 2010a) for the surface (a,d), Atlantic (b,e) and Pacific (c,f) vertical sections. Units are in [$\mu$mol L$^{-1}$].

**Figure s6.** BCM-C simulated and observed (GLODAP, Key et al., 2004) surface distribution of dissolved inorganic carbon (a,d) and alkalinity (b,e). In addition, we plotted here estimates of carbonate ion concentration taken from subtracted DIC from ALK (c,f). Units are in [$\mu$mol kg$^{-1}$].
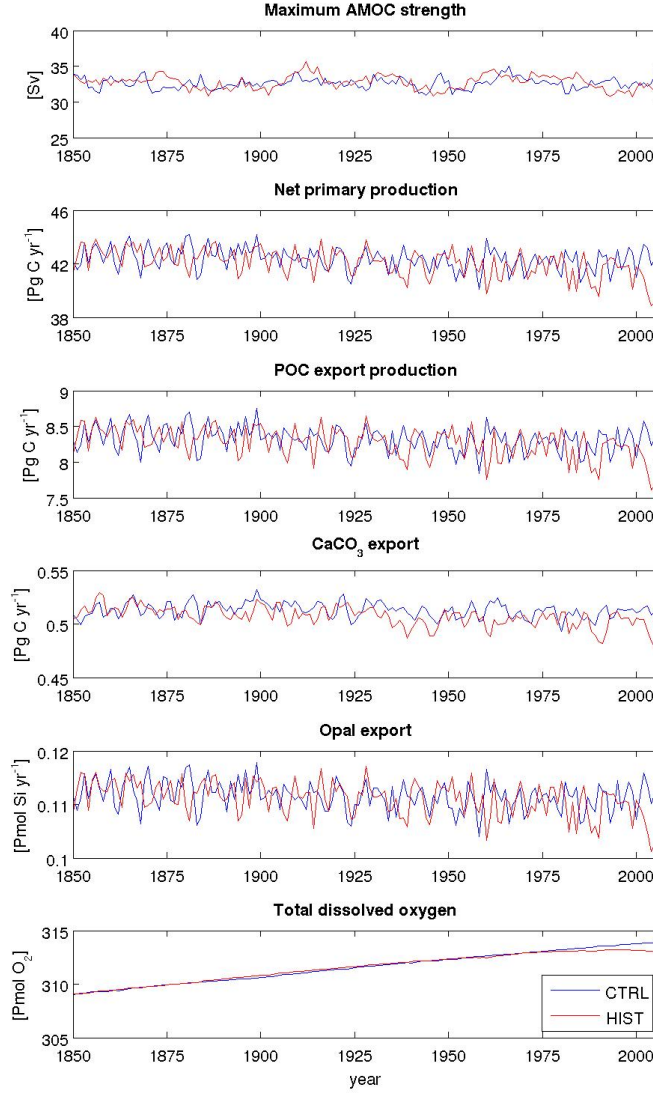
**Figure s7.** Time-series of annual mean maximum Atlantic meridional overturning circulation (AMOC) strength, net primary production, cabon export production, calcium carbonate export, opal export, and oxygen inventory for the 1850–2005 period. Blue lines represent values from CTRL simulation, whereas red lines HIST simulation.